

Solid C₇₀: A molecular-dynamics study of the structure and orientational ordering

Ailan Cheng and Michael L. Klein

Department of Chemistry, University of Pennsylvania, Philadelphia, Pennsylvania 19104-6323

and Laboratory for Research on the Structure of Matter, University of Pennsylvania, Philadelphia, Pennsylvania 19104-6323

(Received 6 April 1992)

Classical constant-pressure molecular-dynamics simulations have been performed for solid C₇₀ using a pairwise-additive atom-atom Lennard-Jones potential that gave a good account of the high-temperature rotator phase of solid C₆₀. The simulation results indicate that freezing of the rotational motion of C₇₀ molecules about the long and short axes occurs at different temperatures. At high temperatures, an orientationally disordered fcc phase is preferred over a hcp lattice. At low temperature, a triclinic phase seems to be favored by the present model, but other structures (space group *Pa*3, and hcp) also have very competitive potential energies. Estimates of the molecular-reorientation times are given. The librational phonon density of states has been studied. As expected, libration frequencies for rotation about the long axis are lower than that about the short axis.

I. INTRODUCTION

The advent of efficient synthesis¹ procedures for macroscopic quantities of fullerenes has led to widespread investigation of the solid-state properties of these systems, especially C₆₀. At room temperature the spheroid-shaped C₆₀ molecules adopt a fcc lattice in which molecules are rotating.²⁻⁶ Upon cooling, an orientational ordered phase is observed below 250 K. The properties of solid C₆₀ have now been well characterized and a clear picture has emerged concerning the structural and dynamical behavior.²⁻¹³ Recent diffraction studies reveal evidence for residual partial disorder in the low-temperature phase.¹³

Solid C₇₀ has received less attention than solid C₆₀. The C₇₀ cluster is ellipsoid shaped. The carbon-atom cage can be thought of as a band of hexagons capped with halves of a C₆₀ molecule.¹⁴ NMR, Raman, and infrared experiments¹⁵⁻²⁰ plus theoretical calculations²¹⁻²⁶ have all confirmed this basic structure. Thus, C₇₀ is composed of 12 pentagons and 25 hexagons which together form an elongated molecule. The two pentagons located at the top and bottom of the molecule are perpendicular to the long axis of the C₇₀ molecule. The narrower midsection of C₇₀ has almost the same cross-sectional diameter as C₆₀, although its fivefold axis is about 1 Å longer than that of the latter. NMR data show that there exist five types of inequivalent carbon atoms.¹⁵⁻²⁰ Theoretical calculations²¹⁻²⁶ indicate that there are eight different bond lengths which can be classified, roughly, as single, intermediate, and double bonds.

Since C₇₀ is ellipsoidal and not spherical like C₆₀, one would expect some differences between them in solid-state properties. For example, the C₇₀ system could perhaps display a very rich phase diagram akin to that of solid N₂.²⁷ Indeed, NMR experiments⁴ indicate that at ambient condition, C₇₀ molecules rotate anisotropically. So far, limited information is available about the structure and orientational ordering. Energy-minimization

calculations predicted a hcp packing of C₇₀ molecules to be more stable than a fcc structure, at zero temperature.²⁸ Early x-ray-diffraction data¹² suggested that solid C₇₀ has a face-centered-cubic structure, and also showed that the C₇₀-pentane fulleride crystal is monoclinic.²⁹ More recent x-ray-diffraction data³⁰ show that the equilibrium phase above room temperature is fcc, but that structural defects as well as residual solvent tend to stabilize the hcp phase. Thus even highly pure C₇₀ samples contain mixed-phase crystals consisting primarily of the fcc phase but also some hcp. In both the fcc and hcp structures the data were well described by a model incorporating complete molecular orientational disorder.

In this paper, we report the results of a molecular-dynamics (MD) study of orientational ordering in solid C₇₀. Several different structures are compared. The simulation results suggest that a low-symmetry triclinic phase achieves a more efficient packing relative to the *Pa*3 and hcp structure, favored by N₂ molecules.²⁷ The rotational motion of the C₇₀ molecule is confirmed to be anisotropic; molecules rotate faster about their long axes at high temperature. C₇₀ molecules are predicted to stop tumbling on the MD time scale at a temperature between 300 and 400 K. However, molecules continue to spin about their long axes. Around 100 K the spinning motion is also frozen on the MD time scale.

II. DETAILS OF THE CALCULATIONS

Since C₆₀ and C₇₀ have similar cohesive energies,³¹ we have adopted the same intermolecular potential used in our study of C₆₀.^{32,33} In that work, the potential energy was assumed to be the sum of pairwise-additive intermolecular interactions, each represented by a sum of C-C Lennard-Jones (12-6) potentials with the parameters ($\epsilon=28$ K and $\sigma=3.4$ Å) taken from a study of graphite.³⁴ The room-temperature structure and compressibility of C₆₀ obtained by using this potential model are in good agreement with experimental data.² The limitation

of this simplistic intermolecular potential for C_{60} has been discussed in a recent article.³³ While orientational freezing occurs in the correct temperature range, the resulting ground-state structure is not consistent with experimental data. The potential model for C_{60} has been improved by incorporating additional interaction sites as well as electrostatic interactions.³⁵ However, the computational time necessarily increases. Since the simple model did so well for C_{60} in the high-temperature rotator phase, we adopted the same model here.

In this work, C_{70} molecules are considered to be rigid with the carbon coordinates taken from quantum-chemistry calculations.²³ With these carbon coordinates C-C bond lengths fall between 1.364 and 1.486 Å, the equatorial cross sectional diameter is 7.092 Å and the spatial extent along the fivefold axis is 7.966 Å. We chose the long axis of the molecule to be the z direction of the principal axis. A standard constant-pressure molecular-dynamics algorithm was used.^{36,37} The equations of motion for translational degrees of freedom were solved by a third-order Gear predictor-corrector algorithm.³⁸ Rotational motion, described by quaternions, was integrated by a fourth-order algorithm. Because of the large number of interaction sites involved in the evaluation of the force and configuration energy, most simulation runs were performed on small systems containing either 32 or 108 C_{70} molecules.

III. SIMULATION RESULTS

Since there is no information on the low-temperature structure available at present, it is difficult to choose an optimal initial configuration. We have therefore compared three obvious initial configurations. (1) Molecular centers on the lattice points of a fcc lattice, with the long axis of all C_{70} molecules pointing along one of the diagonal $\langle 111 \rangle$ directions. (2) A static structure resembling that of a $Pa3$ lattice, in which the molecules are placed at the fcc lattice points and the long axes are arranged along the four appropriate $\langle 111 \rangle$ directions. (3) Molecular centers on the lattice points of a hcp lattice with fivefold axes pointing along the c direction. For simplicity, we will denote the three sets of simulation data as fcc, $Pa3$, and hcp. In fact, during the MD simulations some systems relaxed to a different structure. In this case, the notation we employ only refers to the *initial* configuration of the simulation, rather than the specific symmetry at

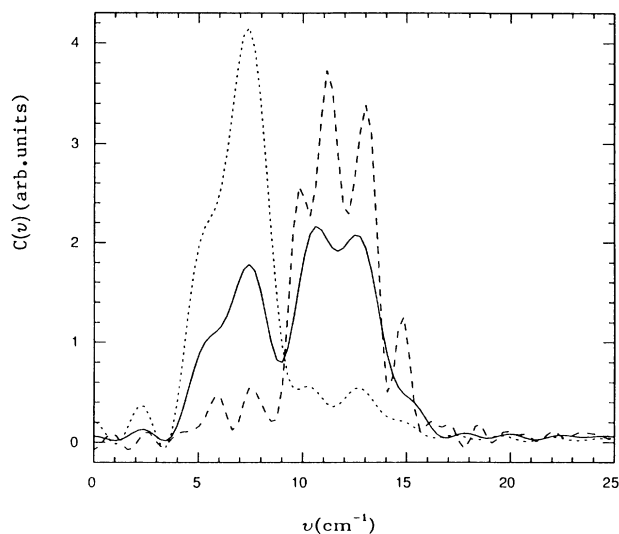


FIG. 1. The librational phonon density of states for a triclinic lattice of solid C_{70} . The solid line is for the total density of states, the dotted line is for the librational motion about a fivefold long axis, and the dashed line is for the libration about a short axis. The intensities are in arbitrary units.

that particular temperature.

As suggested by NMR data,⁴ C_{70} molecules rotate anisotropically under ambient conditions. Here, the rotational motion is monitored by calculating the reorientational relaxation times of the three mutually perpendicular principal axes. Table I gives the estimates of the relaxation times for two of the simulations mentioned above. The rotational motion is not particularly sensitive to the lattice structure: The two sets of data agree with each other surprisingly well, in view of the large statistical uncertainty in evaluating the appropriate time-correlation functions. At 100 K, C_{70} molecules are no longer rotating on the MD time scale. As the temperature increases the molecules first begin to spin about the fivefold (long) axis and above 300 K they start tumbling. Thus, there are two orientational freezing processes corresponding to the freezing of tumbling motion between 300 and 400 K and freezing of spinning about the long axis around 100 K.

In the low-temperature phase, the phonon density of states for the librational motion has two bands. Figure 1

TABLE I. Reorientational relaxation times and orientational order parameters for solid C_{70} in two structures. Typical error for τ_1 and τ_2 is 25%.

Structure	T (K)	τ_1 (ps)		τ_2 (ps)		C_4	C_6
		Long axis	Short axis	Long axis	Short axis		
fcc	107					-1.47	2.08
	326	600	8	200	13	-0.98	1.05
	498	18	5	10	5	-0.26	0.52
$Pa3$	100					-1.46	2.07
	311	300	9	400	6	-0.65	0.82
	521	7	5	7	4	0.04	0.28

shows the density of states for the librational motion for the fcc sample at 100 K (the lattice at 100 K is now actually triclinic; see below). Similar results are found for samples with *Pa3* and hcp structures. The phonon density is calculated by taking the Fourier transformation of the angular velocity correlation function. Strictly speaking, *x* and *y* directions are not equivalent for a C_{70} molecule, but they are very similar so that librational frequencies about these two axes overlap and cannot be resolved. The density of states for the librational motions about the molecular short axis (in the molecular *x-y* plane) and the *z* axis is shown in Fig. 1 also. The low-frequency band corresponds to librational motion about the long axis. As temperature increases, molecules begin to spin about the long axis and the peak frequency systematically shifts to zero.

If the high-temperature phase is cubic, the orientational ordering of the long axis can be described by an orientational distribution function, which in turn can be expressed in terms of the Kubic-harmonic functions.³⁹ The coefficients, C_4 and C_6 , customarily used as orientational order parameters⁴⁰ are given in Table I. Above 400 K, the small values of C_4 and C_6 suggests that C_{70} molecules are oriented randomly. In fact, the analysis of a typical trajectory shows that molecules undergo hindered anisotropic rotations. The anisotropic motion is also justified by the different relaxation times for rotations about long and short axes, respectively. The large positive C_6 and large negative C_4 around room temperature are consistent with preferential $\langle 111 \rangle$ orientation of the long axis.

The symmetry of the lattice is, of course, strongly related to the orientational ordering of the C_{70} molecules. In the case where the MD run was initiated with all molecules initially pointing along a common diagonal of a fcc lattice, the low-temperature crystal spontaneously distorted to a triclinic structure stretched along the fcc $\langle 111 \rangle$ direction. At 100 K, when there is no rotation, the centers of mass of C_{70} in the (111) plane form a slightly distorted triangular lattice as signaled by the small splitting of simulation cell angles. The slight distortion is due to the incompatibility of the fivefold symmetry of the long axis with that of the (111) lattice plane. A snapshot of three adjacent (111) planes suggest that C_{70} molecules are orientationally ordered.

On heating, the C_{70} molecules start to rotate about their long axes, a motion that averages out the fivefold symmetry and leads to a trigonal lattice. When the temperature increases further, the molecules begin to tumble around. This motion, which effectively makes the molecules more spherical, leads to a higher-symmetry phase, namely a fcc lattice, as indicated by the equal cell lengths and 90° cell angles.

When the centers of mass of C_{70} molecules are assigned to a hcp lattice with the fivefold axis of all C_{70} pointing along the *c* direction, the lattice spontaneously distorted. However, the lattice relaxes to ideal hcp when the temperature is sufficiently high that the molecules rotate more or less isotropically.

It is not surprising that the initial *Pa3* structure

remains cubic for all temperatures and simply expands as the temperature is increased. At high temperature, both the *Pa3* and the initial fcc lattice converged to a fcc structure where C_{70} molecules are orientationally disordered.

Unfortunately, the question as to the structure of the ground state remains unanswered by our calculations. A possible structural martensitic transition, between hcp and fcc, is likely inhibited by the periodic boundary conditions in the present simulations. To obtain better statistics on the evaluation of the configuration energy, we carried out lengthy simulations on $3 \times 3 \times 3$ unit-cell systems for the three structures discussed above. With this system we were able to use a larger cutoff (15 Å) for the computation of interactions between pairs of molecules. At 100 K, configurational energies obtained for the triclinic, hcp, and *Pa3* structures, -166.9 , -166.3 , and -165.5 kJ/mol, respectively, are very competitive. The triclinic structure has slightly lower configurational energy relative to the other two lattices. This is consistent with more efficient molecular packing, since the calculated volumes per C_{70} molecule are 814.9 \AA^3 for the triclinic, 815.7 \AA^3 for the hcp, and 817.2 \AA^3 for the *Pa3* structures. The hcp lattice parameters obtained at 100 K are $a = 10.05 \text{ \AA}$, $b = 17.45 \text{ \AA}$, and $c = 18.60 \text{ \AA}$ for a rectangular simulation box in the *x-y* plane. This gives $c/a = 1.795$, which is considerably greater than the ideal hcp value of 1.632. The average cell length of the triclinic structure is 14.92 \AA and the simulation box shears by 5°.

Simulations on the larger system were also performed around 500 K for hcp and fcc lattices. The potential energies obtained were again very competitive for these two structures. The configurational energies for the smaller samples are in good accord with those for large samples. Both sets of data indicate that, energetically, C_{70} favors a triclinic lattice at 100 K and fcc at higher temperature.

IV. CONCLUSIONS

We have presented results of molecular-dynamics simulations on the solid phase of rigid C_{70} molecules based on a simple pairwise-additive atom-atom intermolecular potential. The simulation results suggests that C_{70} molecules freeze into an orientationally ordered phase above 100 K. Spinning about the long axis occurs around 100 K and tumbling motion starts above 300 K. C_{70} molecules undergo relatively rapid anisotropic rotation at higher temperatures. The calculated value of the orientational freezing temperature, between 300 and 400 K, can be compared with the experimental value of 300–350 K.³⁰ The density of librational states is predicted to exhibit two distinct bands of librational modes corresponding to the motion about the long and short axes, respectively. Since the frequency spectrum is very sensitive to the potential model adopted, this calculation will likely provide a rather stringent test of our model. The predicted frequencies are likely lower bounds since electrostatic interactions will almost certainly increase the torsional barrier.

We have identified structural transformations associated with the rotational degrees of freedom of the C₇₀ molecules. As molecular orientational disordering increases, molecules become effectively more spherical and the centers-of-mass structure approaches a fcc lattice. This finding agrees with recent x-ray-diffraction data,³⁰ in which the majority of scattering peaks at high temperature can be indexed to a fcc lattice with a smaller fraction of a hcp component. The calculated fcc lattice constant, 15.1 Å at 400 K, agrees fairly well with the experimental value of 14.96 Å at room temperature. The hcp lattice parameters for the model system at 472 K, $a = 10.4$ Å, $b = 18.1$ Å, and $c = 18.1$ Å, are reasonably consistent with the experimental values $a = 10.56$ Å, $b = 18.29$ Å, and $c = 17.35$ Å at 325 K.

All three structures investigated here have very competitive configurational energies at low temperature. The low-symmetry triclinic phase has a slightly lower energy and achieves more efficient packing compared with the other two structures studied herein. However, the current data seem to disagree with a published energy-minimization calculation²⁸ which suggested that the hcp

lattice is favored over the triclinic phase by 1.47 kJ/mol. We are unable to explain the difference but note that the latter work was carried out by using a model with flexible C₇₀ molecules. One should also keep in mind that the free energy rather than configurational energy should be used as the criterion for judging the stability of a particular structure. Further study, especially in the low-temperature region, with a more refined intermolecular potential, will be necessary to help clarify the experimental situation.

ACKNOWLEDGMENTS

We thank our colleagues at the University of Pennsylvania Laboratory for Research on the Structure of Matter for helpful discussions on fullerites. We are grateful to P. W. Fowler for providing us with the atomic coordinates of the C₇₀ molecule. Special thanks go to Paul A. Heiney and Gavin Vaughan for many useful discussions. This research was supported by the National Science Foundation under Grants No. CHE 87-22481, No. CHE 88-15130, and No. DMR 88-19885.

- ¹W. Krätschmer, L. D. Lamb, K. Fostiropoulos, and D. R. Huffman, *Nature* **347**, 354 (1990); W. Krätschmer, K. Fostiropoulos, and D. R. Huffman, *Chem. Phys. Lett.* **170**, 167 (1990).
- ²J. E. Fischer, P. A. Heiney, A. R. McGhie, W. J. Romanow, A. M. Denenstein, J. P. McCauley, Jr., A. B. Smith III, and D. E. Cox, *Science* **252**, 1288 (1991).
- ³P. A. Heiney, J. E. Fischer, A. R. McGhie, W. J. Romanow, A. M. Denenstein, J. P. McCauley, Jr., A. B. Smith III, and D. E. Cox, *Phys. Rev. Lett.* **66**, 2911 (1991).
- ⁴R. Tycko, R. C. Haddon, G. Dabbagh, S. H. Glarum, D. C. Douglass, and A. M. Muzsca, *J. Phys. Chem.* **95**, 518 (1991).
- ⁵R. Tycko, G. Dabbagh, R. M. Fleming, R. C. Haddon, A. V. Makhija, and S. M. Zahurak, *Phys. Rev. Lett.* **67**, 1886 (1991).
- ⁶C. S. Yannoni, R. D. Johnson, G. Meijer, D. S. Bethune, and J. R. Salem, *J. Phys. Chem.* **95**, 9 (1991).
- ⁷R. Sachidanandam and A. B. Harris, *Phys. Rev. Lett.* **67**, 1467 (1991); P. A. Heiney, J. E. Fischer, A. R. McGhie, W. A. Romanow, A. M. Denenstein, J. P. McCauley, Jr., A. B. Smith III, and D. E. Cox, *ibid.* **67**, 1468 (1991).
- ⁸W. I. F. David, R. M. Ibberson, J. C. Matthewman, K. Prassides, T. J. S. Dennis, J. P. Hare, H. W. Kroto, R. Taylor, and D. R. M. Walton, *Nature* **353**, 147 (1991).
- ⁹D. A. Neumann, J. R. D. Copley, R. L. Cappelletti, W. A. Kamitakahara, R. M. Lindstron, K. M. Creegan, D. M. Cox, W. J. Romanow, N. Coustel, J. P. McCauley, Jr., N. C. Maliszewski, J. E. Fischer, and A. B. Smith III, *Phys. Rev. Lett.* **67**, 3808 (1991).
- ¹⁰P. A. Heiney, G. B. M. Vaughan, J. E. Fischer, N. Coustel, D. E. Cox, J. R. D. Copley, D. A. Neumann, W. A. Kamitakahara, K. M. Creegan, D. M. Cox, J. P. McCauley, Jr., and A. B. Smith III, *Phys. Rev. B* **45**, 4544 (1992).
- ¹¹R. D. Johnson, C. S. Yannoni, H. C. Dorn, J. R. Salem, and D. S. Bethune, *Science* **255**, 1235 (1992).
- ¹²R. M. Fleming, in *Large Carbon Clusters*, American Chemical Society Symposium Series (American Chemical Society, Washington, D.C., in press).
- ¹³W. I. F. David, R. M. Ibberson, T. J. S. Dennis, J. P. Hare, and K. Prassides, *Europhys. Lett.* **18**, 219 (1992); R. Hu, T. Egami, F. Li, and J. S. Lanin (unpublished).
- ¹⁴J. R. Heath, S. C. O'Brien, Q. Zhang, Y. Liu, R. F. Curl, H. W. Kroto, F. K. Tittle, and R. E. Smalley, *J. Am. Chem. Soc.* **107**, 7779 (1985).
- ¹⁵R. Taylor, J. P. Hare, A. K. Abdul-Sada, and H. W. Kroto, *J. Chem. Soc. Chem. Commun.* **20**, 1423 (1990).
- ¹⁶H. Aije, M. M. Alvarez, S. J. Anz, R. D. Beck, F. Diederich, K. Fostiropoulos, D. R. Huffman, W. Krätschmer, Y. Rubin, K. E. Schriver, K. Sensharama, and R. L. Whetten, *J. Phys. Chem.* **94**, 8630 (1990).
- ¹⁷R. D. Johnson, G. Meijer, J. R. Salem, and D. S. Bethune, *J. Am. Chem. Soc.* **113**, 3619 (1991).
- ¹⁸D. S. Bethune, G. Meijer, W. C. Tang, and H. J. Rosen, *Chem. Phys. Lett.* **174**, 219 (1990).
- ¹⁹D. S. Bethune, G. Meijer, W. C. Tang, H. J. Rosen, W. G. Golden, H. Seki, C. A. Brown, and M. S. de Vries, *Chem. Phys. Lett.* **179**, 181 (1991).
- ²⁰D. R. McKenzie, C. A. Davis, D. J. H. Cockayne, D. A. Muller, and A. M. Vassallo, *Nature* **355**, 622 (1992).
- ²¹Z. Slanina, J. M. Rudzinski, M. Togasi, and E. Osawa, *J. Mol. Struct. (Theochem)* **202**, 169 (1989).
- ²²D. E. Manolopoulos, J. C. May, and S. E. Down, *Chem. Phys. Lett.* **181**, 105 (1991).
- ²³P. W. Fowler, P. Lazzeretti, M. Malagoli, and R. Zanasi, *Chem. Phys. Lett.* **179**, 174 (1991).
- ²⁴G. E. Scuseria, *Chem. Phys. Lett.* **180**, 451 (1991).
- ²⁵K. Raghavachari and C. M. Rohlfing, *J. Phys. Chem.* **95**, 5768 (1991).
- ²⁶W. Andreoni, F. Gygi, and M. Parrinello, *Chem. Phys. Lett.* **189**, 241 (1992).
- ²⁷R. LeSar, S. A. Ekberg, L. H. Jones, R. L. Mills, L. A. Schwalbe, and D. Schiferl, *Solid State Commun.* **32**, 13 (1979); D. T. Cromer, R. L. Mills, D. Schiferl, and L. A. Schwalbe, *Acta Crystallogr. Sec. B* **37**, 1 (1981), and references therein.
- ²⁸Y. Guo, N. Karasawa, and W. A. Goddard III, *Nature* **351**, 464 (1991).

- ²⁹R. M. Fleming, A. R. Kortan, B. Hessen, T. Siegrist, F. A. Thiel, O. Marsh, R. C. Haddon, R. Tycko, G. Dabbagh, M. L. Kaplan, and A. M. Muzsca, *Phys. Rev. B* **44**, 888 (1991).
- ³⁰G. B. M. Vaughan, P. A. Heiney, J. E. Fischer, D. E. Luzzi, D. A. Ricketts-Foot, A. R. McGhie, Y. W. Hui, A. L. Smith, D. E. Cox, W. J. Romanow, B. H. Allen, N. Coustel, J. P. McCauley, Jr., and A. B. Smith III, *Science* **254**, 1350 (1992).
- ³¹C. Pan, M. P. Sampson, Y. Chai, R. H. Hauge, and J. L. Margrave, *J. Phys. Chem.* **95**, 2944 (1991).
- ³²A. Cheng and M. L. Klein, *J. Phys. Chem.* **95**, 6750 (1991).
- ³³A. Cheng and M. L. Klein, *Phys. Rev. B* **45**, 1889 (1992).
- ³⁴W. A. Steele, *The Interaction of Gases with Solid Surfaces* (Pergamon, New York, 1974); L. A. Girifalco, *J. Phys. Chem.* **96**, 858 (1992).
- ³⁵M. Sprik, A. Cheng, and M. L. Klein, *J. Phys. Chem.* **96**, 2027 (1992).
- ³⁶M. Parrinello and A. Rahman, *Phys. Rev. Lett.* **45**, 1196 (1980); *J. Appl. Phys.* **52**, 7182 (1981).
- ³⁷S. Nosé and M. L. Klein, *Mol. Phys.* **50**, 1055 (1983); R. W. Impey, M. Sprik, and M. L. Klein, *J. Chem. Phys.* **83**, 3638 (1985).
- ³⁸C. W. Gear, *Numerical Initial Value Problems in Ordinary Differential Equations* (Prentice-Hall, Englewood Cliffs, NJ, 1971).
- ³⁹W. R. Fehlner and S. H. Vosko, *Can. J. Phys.* **54**, 2159 (1976).
- ⁴⁰A. Cheng, M. L. Klein, and L. J. Lewis, *Phys. Rev. B* **44**, 13 (1991).